JOURNAL OF SPACECRAFT AND ROCKETS
Vol. 32, No. 6, November–December 1995

Roll Damping for Projectiles Including Wraparound, Offset, and Arbitrary Number of Fins

Ameer G. Mikhail*
U.S. Army Research Laboratory, Aberdeen Proving Ground, Maryland 21005-5066

An algebraic correlation for the roll-damping and roll-producing moments for finned projectiles and missiles has been extended and verified to accept bodies with an arbitrary number of fins—not only cruciform fins, but curved wraparound fins with fin cant, and fins with offset angles. The extended correlation is applicable at subsonic, transonic, and supersonic speeds. A direct method to compute the fin roll-producing moment from the fin normal force is provided to circumvent the existing lengthy and cumbersome semiempirical methods. Seven different missile and projectile configurations with widely varying fin shapes and sizes were tested, and their measured data are tabulated. The present correlation is very simple, and can be used to refine initial configuration selection and thus reduce the number of costly full-flowfield computations. The correlation is limited to missiles with only one set of fins and to small angles of attack.

Nomenclature

A_{ref} = reference area, $\pi d^2/4$
B = fin panel offset angle, deg
C_D = drag coefficient, drag force/$(q_\infty A_{ref})$
C_l = rolling-moment coefficient, $l/(q_\infty A_{ref} d)$
C_{lp} = roll-damping-coefficient derivative, $\partial C_l/\partial(pd/2V)$, per radian
$C_{l\delta}$ = roll-producing moment coefficient derivative, $\partial C_l/\partial\delta$, per radian
C_N = normal-force coefficient, normal force/$(q_\infty A_{ref})$
$C_{N\alpha}$ = normal-force slope coefficient, $\partial C_N/\partial\alpha$, per radian
C_{NFi} = normal-force coefficient for fin panel i
d = reference diameter
h = distance between chord endpoints for curved fin panels
I_x = axial (polar) moment of inertia about the body geometrical (spin) axis
l = roll moment; also curved-fin chord length
M = Mach number
m = exponent in the new correlation of Eq. (5)
n = number of canted panels in a fin set
p = spin rate of projectile, rad/s except when otherwise noted in Hz
p_s = steady-state roll (spin) rate
q = dynamic pressure, $0.5\rho V^2$
V = projectile velocity
y_c = radial distance from fin area center to projectile axis
α = angle of attack
δ = fin cant angle for a whole fin panel (deflection angle)
δ_p = partial fin cant angle (chamfer) at the leading and/or trailing edge of the fin panel
δ_{eq} = equivalent whole-panel fin cant angle for the partially canted (chamfered) fin
ρ = air density
ϕ = roll angle, rad
$\dot{\phi}$ = roll (spin) rate, $\partial\phi/\partial t$, rad/s except when otherwise noted in Hz
$\ddot{\phi}$ = $\partial\dot{\phi}/\partial t$

Subscript

∞ = freestream condition

Presented as Paper 93-3460 at the AIAA Applied Aerodynamics Conference, Monterey, CA, Aug. 9–11, 1993; received Sept. 1, 1993; accepted for publication June 23, 1995.

*Aerospace Engineer, Propulsion and Flight Division, Weapons Technology Directorate. Associate Fellow AIAA.

I. Introduction

THE roll-damping coefficient is needed to compute the rolling motion and history and to estimate the steady-state spin rate for projectiles and missiles. One also needs to know the corresponding fin-produced rolling-moment coefficient $C_{l\delta}$, which is easier to measure in wind tunnels or compute with analytie and empirical formulas. The roll-damping moment coefficient, on the other hand, is much more difficult to measure and requires a free-spinning rig in association with a sting balance. The roll-damping moment can also be deduced from the free flight motion in an instrumented firing range by recording the projectile spin history using a marking point (usually a base pin) and data reduction of spark shadowgraph film plates. Therefore, a method to adequately estimate the roll-damping moment coefficient C_{lp} is needed.

Eastman[1] observed the algebraic relation provided by Bolz and Nicolidas[2] and applied the theoretical expression of Adams and Dugan,[3] only to find that it did not fit the array of configurations it was applied to. Eastman then empirically established his correlation and showed that it fitted the experimental data well. Eastman's correlation was declared valid only for bodies with four fins in cruciform (i.e., plus, +) formation, because it had its roots in Adams and Dugan's analysis. However, the empirical change that Eastman made should have removed that restriction, except for the fact that Eastman never applied the correlation to any fin setting other than the cruciform formation. In recent efforts, a need has arisen for estimating the roll damping for curved wraparound fins and for fin sets with three or six fin panels. The effect of the curved fin surfaces and the arbitrary number of fins had to be addressed. In addition, it was not known whether the earlier correlation would hold true for offset fins (those mounted at an angle other than 90 deg with the body circumferential tangent line, as shown in Fig. 1).

Analytical and semiempirical methods[3–6] are used in the literature to estimate C_{lp} and/or $C_{l\delta}$. Difficulties arise from the need to identify the assumptions and limitations of each analysis or empirical method, so one knows in advance if the fin configuration and the number of fin panels are acceptable. Also, very often, only supersonic speed regimes are considered, on account of the relative ease in utilizing the linearized supersonic theory. Thus, transonic and subsonic applications are seldom studied.

The present extended correlation takes advantage of the more available and usually more accurate values of $C_{l\delta}$ (whether measured or computed) to evaluate the more difficult to measure and usually elusive C_{lp}. The present correlation is applicable for a wider range of configurations than all earlier relations. Application to configurations with six fins indicated the validity of the correlation to configurations other than four-panel cruciform fins. Application to fins with offset angles between 45 and 135 deg also confirmed the validity of the correlation for that fin type. Finally, the effect of fin

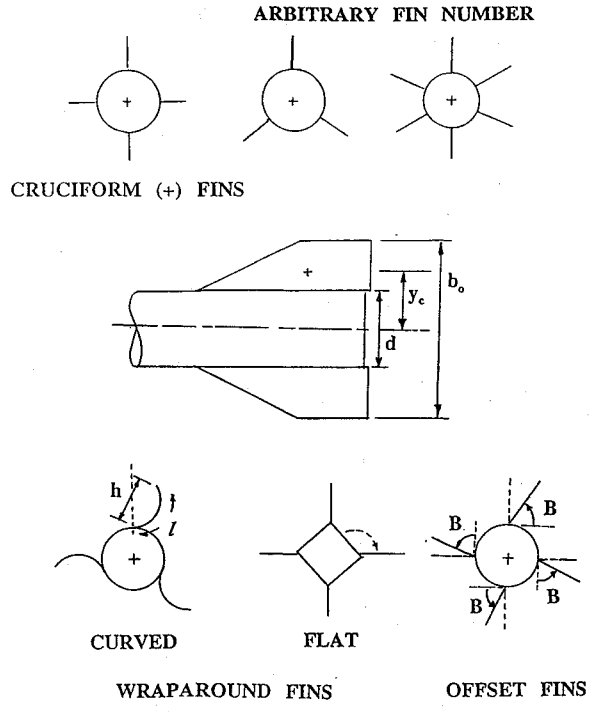

Fig. 1 Nomenclature for fin arrangements.

panel curvature in a three-panel curved wraparound fin configuration is also included in the extended correlation.

An approximate engineering method for estimating $C_{l\delta}$ from the fin C_N is presented, and proved to be surprisingly more accurate than the more widely used semiempirical method of Ref. 7.

II. Analysis

To understand and explain the present correlation, one has to discuss its origin and relation to the equation for the pure rolling motion of symmetric missiles. The analysis and justification of the extended correlation are discussed next.

A. Equation of Pure Rolling Motion

The equation of rolling motion about the body axis is usually written as

$$\left(C_{l\delta}\delta + C_{lp}\frac{pd}{2V}\right)q_\infty A_{\text{ref}}d = I_x\ddot{\phi} \tag{1}$$

where the roll-producing moment coefficient C_l due to the fin cant angle δ is usually written as the coefficient derivative $C_{l\delta}$ multiplied by the cant angle δ (linearity assumed). The opposing linear moment (damping moment) is usually written as the product of the coefficient derivative C_{lp} times $pd/2V$. Note that in the present work, as in Ref. 1, C_{lp} is defined as

$$X = \frac{\partial C_l}{\partial(pd/2V)}$$

Also, $p = \dot{\phi}$ = the roll rate. The damping (opposing) roll moment derivative coefficient, C_{lp}, has a negative sign, as will be observed.

For the steady-state roll motion, $\ddot{\phi} = 0$ and therefore

$$(C_{lp}/C_{l\delta}) = -2(V\delta/p_s d) \tag{2}$$

Note that if $C_{lp}/C_{l\delta}$ is to be constant (with time), then p_s (the steady-state roll rate) must vary identically with the velocity along the trajectory. However, for projectiles (unpowered), the velocity decreases. Thus, p must also decrease so as to keep the ratio $C_{lp}/C_{l\delta}$ constant. Therefore, if p decreases, then true steady-state roll does not exist. If the ratio of C_{lp} to $C_{l\delta}$ is constant along the trajectory, then that does not translate to a true steady-state spin value, and vice versa.

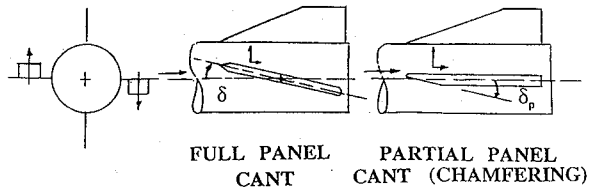

Fig. 2 Fin cant (deflection) angle δ.

Bolz and Nicolidas[2] found, after their range testing of the Basic Finner projectile, that the ratio $C_{lp}/C_{l\delta}$ is independent of Mach number. However, they also called this ratio, erroneously, the "steady state fin tip helix angle per cant angle" because their steady state referred to the 600-ft-long range measurement where the velocity of the projectile does not significantly decrease, and thus the velocity is taken as constant at its midrange value.

B. Cant Angle and Equivalent Cant Angle

Originally, the cant angle δ referred to the angle between the body axis and the chord line of the cross section of the whole fin panel, as depicted in Fig. 2. All (or some) fin panels are deflected in one direction as needed. For a cruciform fin setting, one panel leading edge will be up while the 180-deg-opposite fin panel will have its leading edge down, causing an opposite fin normal force to form the rolling moment l. However, most present-day projectile fins are only partially canted, i.e., the fin cross-section chord line is still parallel to the body axis, with only the leading or/and trailing edge being chamfered at an angle to the fin chord line. This is done for two reasons. First, the whole-panel deflection may be producing too much spin: even though a very small whole-panel cant (of order 0.1 deg) may be possible, it is usually not recommended because the manufacturing errors are then relatively large. Second, the manufacturing cost and accuracy are improved for partial canting (chamfering), while the fin chord remains aligned with the body axis. For projectile applications with fins partially canted, an equivalent whole-fin-panel cant angle δ_{eq} must be determined and used if $C_{l\delta}$ is to be evaluated from the measured value of C_l.

C. Correlation of Eastman

Bolz and Nicolidas[2] published their results in 1950. Adams and Dugan[3] followed in 1958 by publishing their supersonic analysis using the linearized perturbation theory for slender bodies. They extended a two-wing airplane configuration analysis to a four-fin body in the + formation (i.e., cruciform fins). For the cruciform fins they obtained the expression

$$(C_{lp}/C_{l\delta}) = -0.627(d/b_0) \tag{3}$$

where b_0 is the total span of two fin panels including the centerbody diameter. Unfortunately, they never applied this result to any configuration or compared it with any data. Eastman[1] applied Adams and Dugan's expression to several configurations for which data existed for both C_{lp} and $C_{l\delta}$, to find out that their result did not hold true. From these experimental data for C_{lp} and $C_{l\delta}$, Eastman empirically wrote the following correlation in a form similar to the result of the analysis of Adams and Dugan:

$$(C_{lp}/C_{l\delta}) = -2.15(y_c/d) \tag{4}$$

where y_c is the distance between the body roll axis and the area center of one fin panel. Eastman showed that his correlation was valid not only for supersonic speeds as Adams and Dugan's analysis implied, but rather for all speed regimes. Eastman, however, wrongly limited his correlation to cruciform fin configurations, since he thought that the changes he made to Adams and Dugan's expression were minor and that therefore the limitations of their analysis still held. Eastman never applied the correlation to noncruciform fins or to a number of fins other than four. This issue is addressed in detail in Sec. III.

D. Extension to an Arbitrary Number of Fins

Eastman's empirical correlation, Eq. (4), does not come close in numerical value to that of Adams and Dugan, Eq. (3). Although

Eastman had started with Adams and Dugan's expression, he ended up with an expression, though similar in form, that was unrelated to the outcome of their analysis. Therefore, Eastman's expression should not be restricted to Adams and Dugan's limitation of being derived for cruciform fins only. Equation (4) is purely empirical and does not depend on Adams and Dugan's analysis. Having established this fact, the main question left was to investigate how well the data are fitted by the new prescribed correlation of Eq. (4) for fin numbers other than four. In the present work two configurations were considered: one with six fins and another with three fins. Both cases satisfactorily verified the correlation of Eq. (4). These results are discussed in Sec. III.

E. Extension to Curved, Canted Wraparound Fins

Projectiles with curved wraparound fins with no cant angles are known to suffer a reversal in roll direction in the Mach-number range between 1.0 and 2.0, even at low α. Although this behavior is not completely understood, it is generally believed to be due to the intersection of the fins' leading-edge shock waves and their impingement on the rear fin surface, or their just altering the flowfield between the fins so as to produce rolling moment in the opposite direction. In addition, with no intentional cant angle, fin manufacturing tolerances (of order ± 0.05 deg) can also have an influence. Uncanted wraparound fins may have C_l values from $+0.05$ to -0.05. The present analysis will only consider canted wraparound fins (i.e., those that have intentional cant angles) where there is no reversal in roll direction. When analyzing the curved wraparound fin, the fin roll-resisting moment is expected to be larger than that for a similar flat fin with the same fin projected area. This is due to the larger air mass that the fin has to push so that it can move. However, the roll-producing moment may not increase over that of the corresponding flat fin panel. If a correlation similar to Eq. (4) is to exist for this case, C_{lp} must be reduced by a factor related to the curvature of the fin panel. Also, this factor must recover the value 1.0 for the correlation to be valid for noncurved fins as well. The form for the reducing factor C_{lp} was chosen as $(l/h)^m$, where m is an exponent that varies with Mach number to reflect the fin leading-edge shock-intersection effects, and l/h is the ratio of the arc length of the curved fin chord to the distance between the two fin endpoints, as shown in Fig. 1. The exponent m was found to vary with M as $0.1(1 + M + \frac{2}{3}M^2)$, based on the experimental data of C_{lp} and $C_{l\delta}$ of Ref. 10.

Thus, the new extended correlation is written as

$$\frac{C_{lp}}{C_{l\delta}(y_c/d)(l/h)^m} = -2.15 \tag{5}$$

Note that for flat fins, $(l/h)^m$ is equal to 1.0 and the new correlation reduces to the form of Eq. (4). The applied case of Ref. 10 is discussed in Sec. III.

F. Extension to Projectiles with Offset Fins

There has been renewed interest in configurations with offset fins. Offset fins are those erected at an angle B to the tangent to the missile body cross section, as depicted in Fig. 1.

One would expect that the rolling moments for offset fins with B greater than 60 deg would not be greatly less than in the usual 90-deg case. However, one also expects that for B less than 45 deg a large decrease in both $C_{l\delta}$ and C_{lp} will occur. It remains to investigate whether C_{lp} and $C_{l\delta}$ will vary with B in a manner such that their ratio, as prescribed by the general correlation of Eq. (5), remains constant.

Recent range firing data for the Ballistic Research Laboratory (BRL) research projectile were reported by Kayser.[11] Both C_{lp} and $C_{l\delta}$ were measured for rectangular fins at offset angles of 45 and 90 deg. The results of the application are given in Sec. III.

G. Fast Evaluation of $C_{l\delta}$

It is obvious from Eq. (5) that to determine C_{lp} one needs the value of $C_{l\delta}$. Several analytical,[3] semiempirical,[7] and computer codes[7,8] are available in the literature to estimate it. None of these methods is direct, accurate, or valid for all speed regimes. Each method has its limitations and regime of validity. It is difficult from the documentation on each method to pin down all its assumptions or its empirical basis.

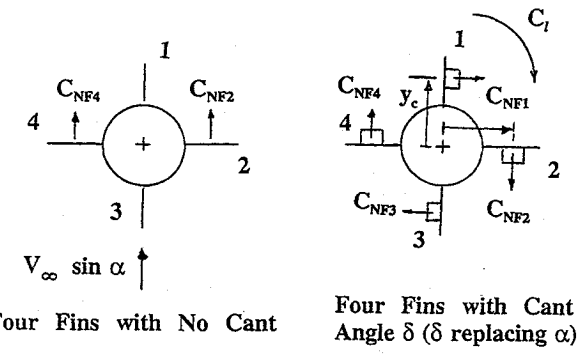

Fig. 3 Nomenclature for estimating $C_{l\delta}$ from C_N.

A suggested simple method that will suffice for most cases is therefore presented here. It is based on the more readily known normal-force slope coefficient, $C_{N\alpha}$, for the fins. This coefficient is readily and routinely computed from fast aerodynamics prediction codes such as those of Refs. 7 and 8. It is computed with no spin effect included. In the present work, the code of Ref. 7 was used to estimate C_N from $C_{N\alpha}$. Linearity in α is assumed, and application is therefore limited to small angles of attack.

As shown in Fig. 3, for a cruciform fin arrangement at an angle of attack α but at no cant (deflection) angle δ, only fin panels 2 and 4 will produce normal force as presented by C_{NF2} and C_{NF4}. Therefore, from the total nonspinning-body computations of the code of Ref. 7, the fin normal force (including both the body–fin and fin–body interferences) is computed by subtracting the body-alone normal force from the total configuration normal force:

$$C_{NF2} = C_{NF4} = \frac{C_{N\text{total config}} - C_{N\text{body alone}}}{2} \tag{6}$$

The factor of 2 in the above equation reflects a one-fin-panel contribution in a four-panel fin configuration, as computed using the code of Ref. 7.

Now, considering the spinning case, with no angle of attack α but with the four fin panels wholly deflected by an angle δ ($\delta = \alpha$), one can easily compute the roll-producing moment C_l as

$$C_l = nC_{NF2}y_c/d \tag{7}$$

Once C_l is computed, $C_{l\delta}$ is simply computed as C_l/δ, assuming that δ is less than 10 deg.

The only approximation in Eq. (7) is the use of y_c, which refers to the fin area center rather than the fin pressure center, as it should theoretically be. However, the fin semispan is usually of order of one body diameter, and therefore the difference between the area and pressure centers is usually small (of the order of 5%).

One major advantage of using Eq. (7) is the inclusion of the effect of the fin–body and body–fin interference effects through the computed C_{NF2}. This effect is large (can be 30% of the fin-alone normal force) and is included by using the code of Ref. 7. Other methods[4–6] are less accurate, owing either to failure to include these effects or to the inadequate estimates of their values if they are included. The error due to using y_c instead of y_{cp} results in much smaller effect than neglecting or miscalculating these interference effects. An example of application of this present approach to the Basic Finner projectile and comparison with other methods for calculating $C_{l\delta}$ is given in the next section.

III. Results of Application to Different Configurations

Following are the results of applying the extended correlation of Eq. (5) to seven different configurations. These seven cases include four cases included in Ref. 1; however, details of the fins are provided herein together with all the tabulated experimental data to furnish a complete archival dataset for future use and verification.

A. M829 Kinetic Energy Projectile (Arbitrary Number of Fins)

This is a subcaliber, saboted projectile fired from a 120-mm smooth-bore gun. It is launched at a speed of 5800 ft/s (1767.7 m/s). The configuration has six fins and a reference diameter of 27 mm (1.065 in.) and is depicted in Fig. 4.

Range data were collected for 11 shots fired. The value of an equivalent angle, δ_{eq}, for a whole panel was estimated,[9] based on detailed fin drawings, to be 0.55 deg. The range data and the present prediction for C_{lp} are provided in Table 1. The listed C_{lp} range values were divided by 2 to conform to the $pd/2V$ notation. In Fig. 4, the C_{lp} values computed from the correlation at the same Mach number were averaged to provide a single value. The individual values, however, are provided in Table 1. Figure 4 indicates that for a six-fin configuration the correlation proved to be valid without any adjustment. Therefore, Eastman's limitation to four cruciform fins is not justified and can be removed.

B. HYDRA 70-mm MK66 Army Missile (Curved Wraparound and Arbitrary Number of Fins)

The U.S. Army 70-mm (2.75-in.) HYDRA MK66 missile is shown in Fig. 5. It has three wraparound fins with partial fin cant. The main body with its rocket motor can carry different warhead configurations. A combination of wind-tunnel and flight testing was made,[10] and the data are given in Table 2. This case was used to establish the fin-curvature correction of Eq. (5). Figure 5 gives the comparison between the present correlation constant of 2.15 and that obtained from the original experimental data. The largest deviation is observed in the range between $M = 1$ and $M = 2$. The agreement gets much better above $M = 2$. The Mach-number correction model for the leading-edge shock-intersection effect proved to be adequate. Notice the lack of the fin shock-intersection effect in the earlier Eastman's correlation result. This effect led to an error in C_{lp} as high as 30% underprediction at $M = 3$, as shown in Fig. 5. Noted also is the application in this case to three fins despite the four-fin restriction of Ref. 1. Therefore, the present correlation of Eq. (5) has been shown to be valid for an arbitrary number of fins, as was also shown in the previous application to the six fins of the M829 projectile.

C. BRL Research Projectile (Offset Fins)

This projectile is a scaled-down model of 40-mm (1.57-in.) in diameter and of length-to-diameter ratio 10. Its model is shown in Fig. 6. It was test fired at BRL (now Army Research Laboratory, ARL) from a 105-mm rifled gun tube, using a discarding sabot. Three models with different fin shapes were tested. The first was a quarter-ellipse (approximately) fin planform. The second was rectangular, and the third was a clipped delta (trapezoid). All these sets of fins had four fin panels. The clipped delta was tested at both 90- and 45-deg offset angles. Range firings for 15 projectiles were reported, including cant angles of 2 and 0.2 deg. Five rounds of the 15 were fired for the 0.2-deg cant and are excluded from the present study because the values of $C_{l\delta}$ are very small and undependable, especially in view of the manufacturing accuracy for a 0.2-deg cant angle, which can be off by 50%. The wiggly result for the C_{lp} of

Table 1 Data and results for the M829 projectile

Mach number	$C_{l\delta}$ (data)	C_{lp} (data)	C_{lp} [Eq. (5)]
3.50	9.85	−18.04	−20.44
3.53	16.35	−32.28	−33.90
3.57	8.23	−16.14	−17.06
3.98	11.49	−22.68	−23.83
4.02	11.48	−19.46	−23.80
4.64	10.83	−25.30	−22.47
4.64	8.61	−19.26	−17.86
4.67	10.19	−21.92	−21.13
5.25	11.34	−20.38	−23.52
5.26	8.80	−17.40	−18.25
5.27	9.30	−21.72	−19.29

Table 2 Data and results for the HYDRA 70-mm MK66

Mach number	$C_{l\delta}$ (data)	C_{lp} (data)	C_{lp} [Eq. (5)]
0.0	2.92	−5.60	−5.65
0.6	2.98	−6.10	−5.94
0.9	3.09	−6.40	−6.29
1.0	3.21	−6.90	−6.55
1.1	3.49	−7.80	−7.22
1.15	3.67	−8.05	−7.63
1.3	4.01	−8.15	−8.45
1.6	3.90	−8.00	−8.46
1.9	3.49	−7.60	−7.84
2.2	3.09	−7.10	−7.21
2.5	2.81	−6.70	−6.85
3.0	2.29	−6.00	−6.04

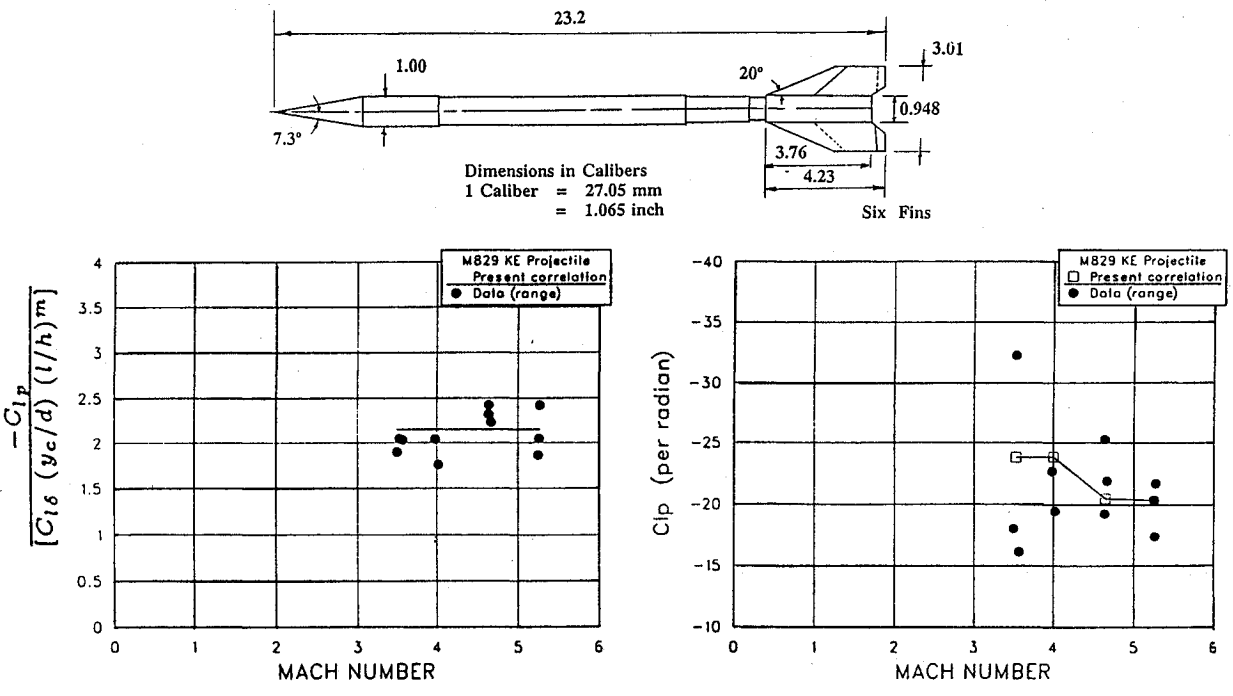

Fig. 4 Geometry, validation, and application to the M829 kinetic energy projectile.

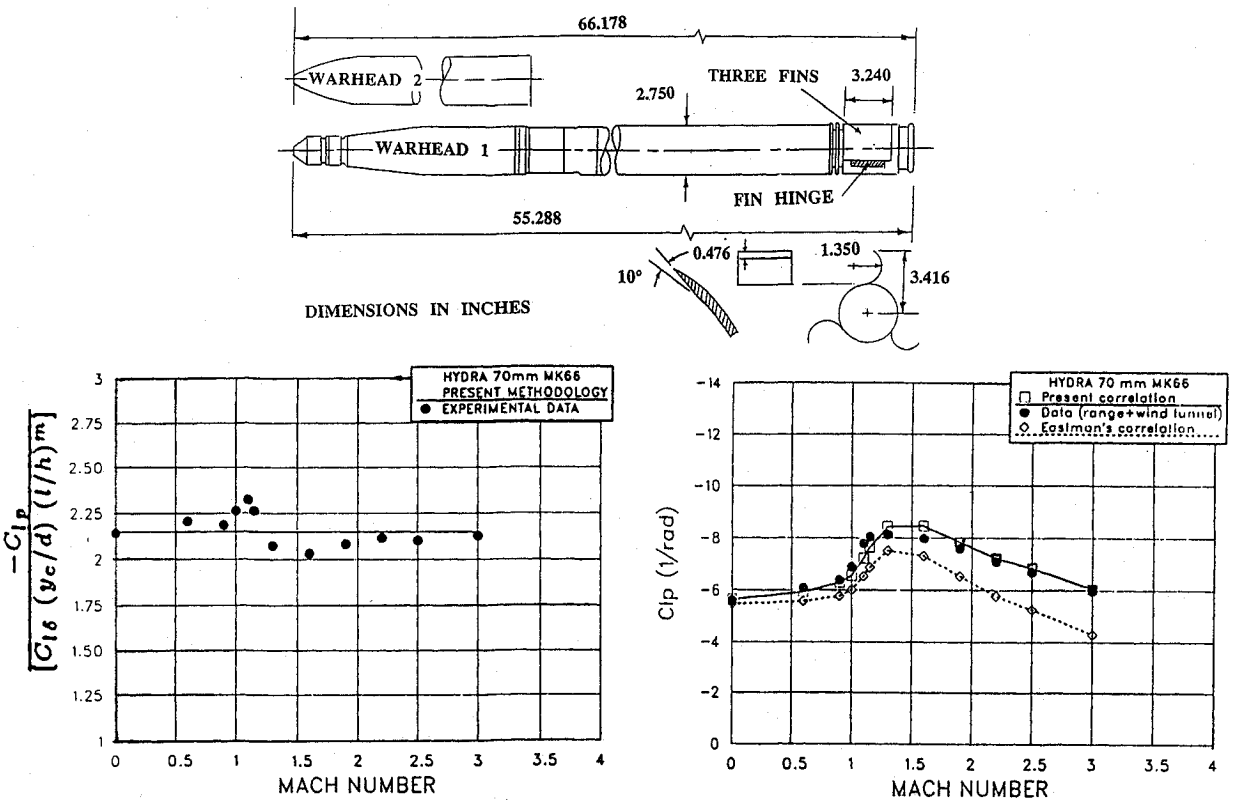

Fig. 5 Geometry, validation, and application to the HYDRA 70-mm MK66 missile.

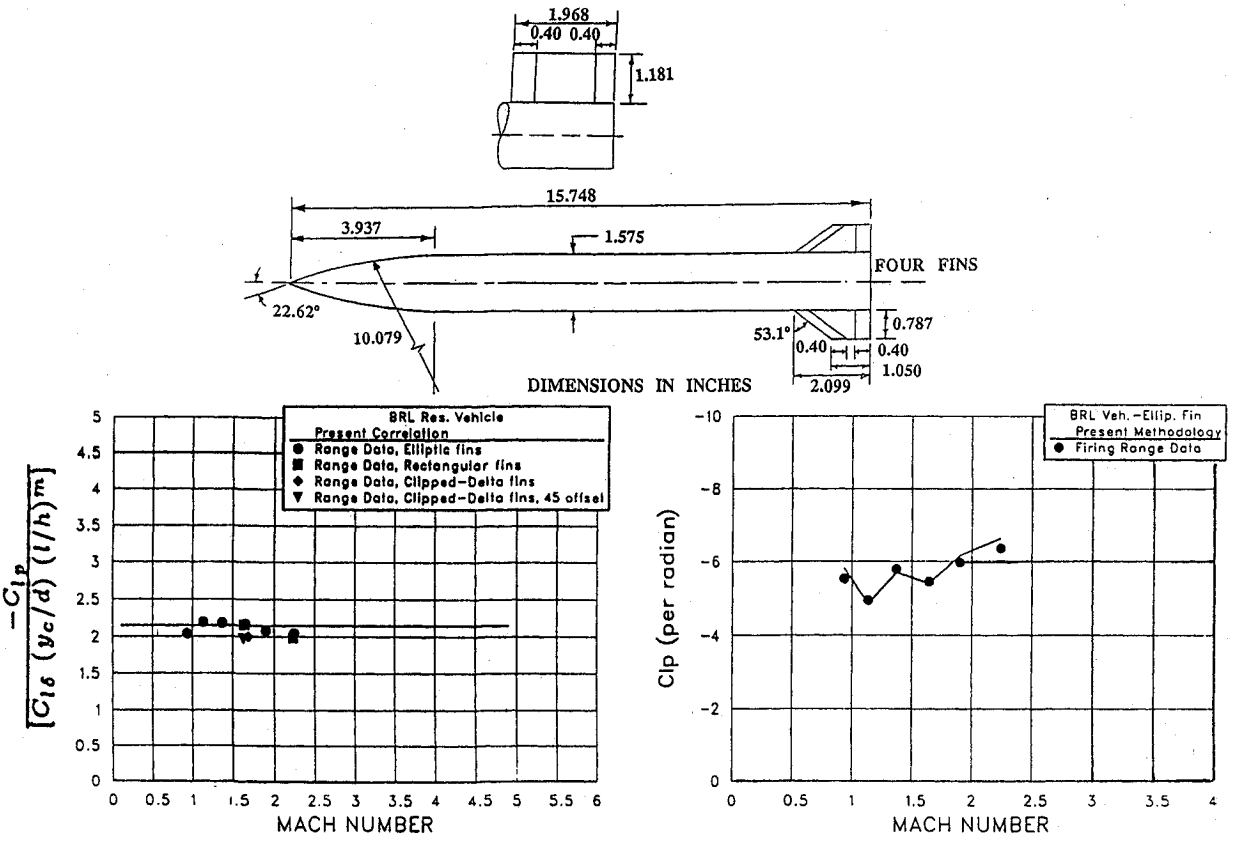

Fig. 6 Geometry, validation, and application to the BRL research projectile.

Fig. 6 for the elliptical fins reflects the use of the corresponding experimental values of $C_{l\delta}$ in Eq. (5).

The clipped-delta fin with 45-deg offset angle provided only about 70% of the C_{lp} and $C_{l\delta}$ of the corresponding 90-deg-offset-angle case, but the ratio of these two coefficients still followed the present correlation of Eq. (5) without any required change, as also shown in Fig. 6.

Thus, it is concluded that for fin offsets greater than or equal 45 deg (up to 135 deg), the present correlation is valid. The results are given in Table 3. Notice that the range data for C_{lp} were divided by 2 to conform to the $pd/2V$ definition.

The following cases (Secs. III.D–III.G) are presented to confirm the exact data and configurations that the earlier work of Ref. 1 had reported. Note that the present correlation of Eq. (5) will reduce

to Eastman's form for any flat fin ($l/h = 1.0$), for any Mach number.

D. Terrier-Recruit First-Stage Vehicle

This is a vehicle of 18-in. (457.2-mm) diam with about 27.5-ft length (90.23 m), as depicted in Fig. 7. It has four simple flat fin panels. Wind-tunnel tests were performed and are reported in Ref. 12. Data are given for speeds between $M = 0.1$ and $M = 5.0$.

Table 3 Data and results for the BRL research projectile

Mach number	Fin planform (offset angle, deg)	$C_{l\delta}$ (data)	C_{lp} (data)	C_{lp} [Eq. (5)]
1.632	Clipped delta (45)	2.35	−3.14	−33.38
1.683	Clipped delta (90)	3.15	−4.74	−5.01
1.633	Rectangular	10.64	−10.66	−10.61
2.227	Rectangular	3.57	−6.22	−6.72
0.934	Elliptical	3.57	−5.54	−5.83
1.134	Elliptical	2.97	−4.96	−4.85
1.370	Elliptical	3.49	−5.80	−5.70
1.643	Elliptical	3.31	−5.46	−5.41
1.899	Elliptical	3.77	−5.98	−6.16
2.241	Elliptical	4.07	−6.34	−6.62

Table 4 Data and results for the Terrier-Recruit first-stage vehicle

Mach number	$C_{l\delta}$ (data)	C_{lp} (data)	C_{lp} [Eq. (5)]
0.1	14.88	−44.84	−45.02
0.5	16.03	−48.19	−48.49
0.8	17.60	−53.21	−53.23
1.0	19.39	−58.57	−58.64
1.16	21.17	−63.92	−64.03
1.5	19.70	−59.57	−59.59
1.8	16.03	−49.19	−48.49
2.4	10.79	−32.46	−32.67
3.5	8.38	−25.43	−25.36
4.0	7.75	−23.42	−23.45
4.5	5.75	−17.40	−17.42
5.0	4.19	−12.72	−12.68

The correlation providing the value of 2.15 was extremely accurate for this case, as shown in Fig. 7. The predicted C_{lp} also is in extremely good agreement with the measured values. The results are also given in Table 4. Note that both $C_{l\delta}$ and C_{lp} of the data presented here were adjusted for the reference length to be based on the vehicle diameter, rather than the total length of the vehicle as was given in Ref. 12.

E. GSRS Boeing Rocket

This Boeing modified General Support Rocket System (GSRS) is shown in Fig. 8. It has a 230-mm (9-in.) diam and four rectangular flat fins, all of which are wholly canted at 0.95 deg for the later version of the rocket described here and in Ref. 13. The body has a 4-deg boattail for the rocket motor nozzle. Wind-tunnel tests results were also reported in the same reference. The experimental data showed some scatter from the extended correlation value of 2.15, as seen in Fig. 8. In particular, the values at $M = 0.7$ for the measured C_{lp} seem to be higher than expected and do not conform to the pattern that C_{lp} decreases with the lowering of Mach number in the transonic and high subsonic speed regimes. Note that the data values in Table 5 were adjusted to refer to a diameter of 230 mm, rather than to 210 mm as used in Ref. 14.

F. Air Force 2.75-in. (70-mm) Folding-Fin Rocket

This rocket, of 2.75-in. (70-mm) diam, has four folding fins that deploy after firing. Figure 9 provides the general configuration. The fins are deployed at a 45-deg angle to the body axis. The fins are partially canted only at the tip to produce rolling moment. A later

Table 5 Data and results for the GSRS Boeing rocket

Mach number	$C_{l\delta}$ (data)	C_{lp} (data)	C_{lp} [Eq. (5)]
0.7	1.99	−3.70	−3.16
0.9	2.26	−3.52	−3.60
1.2	1.68	−2.85	−2.67
1.3	1.95	−3.13	−3.10
1.5	2.49	−3.67	−3.97
2.0	2.53	−3.85	−4.03
3.0	1.95	−2.99	−3.10

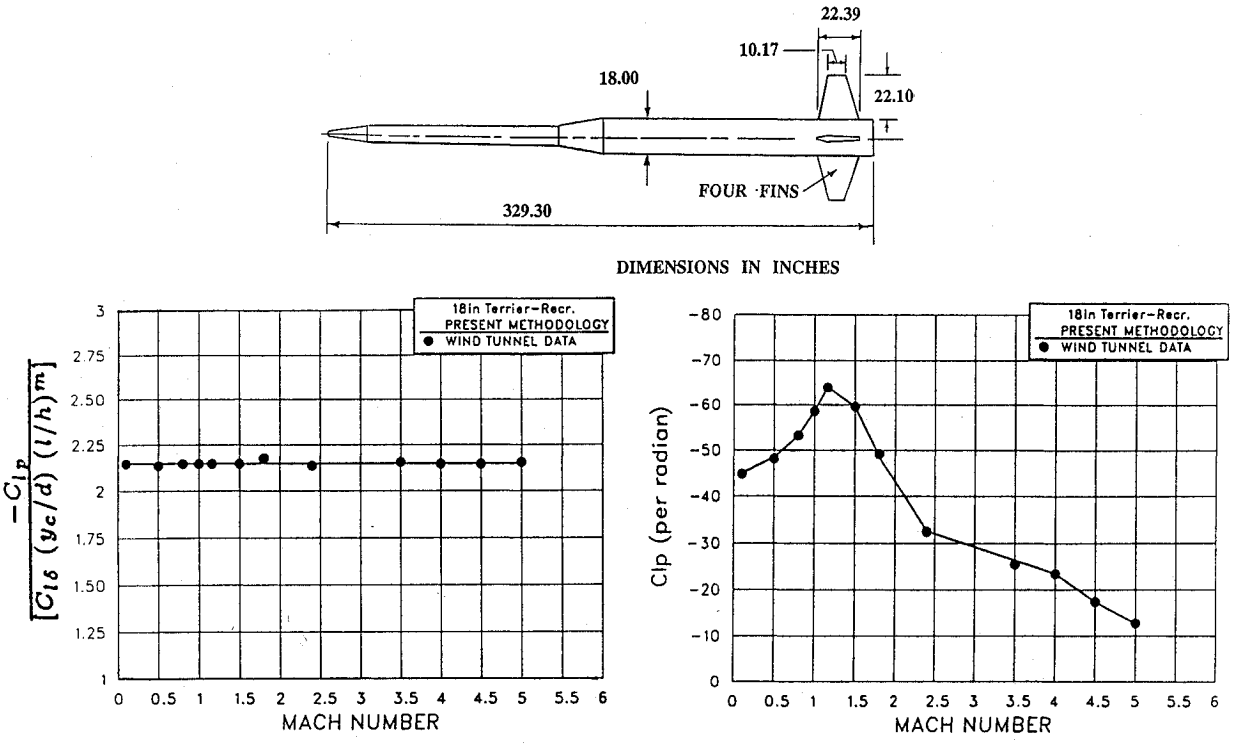

Fig. 7 Geometry, validation, and application to the Terrier-Recruit first-stage vehicle.

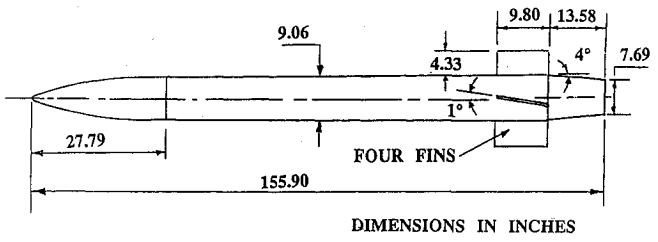

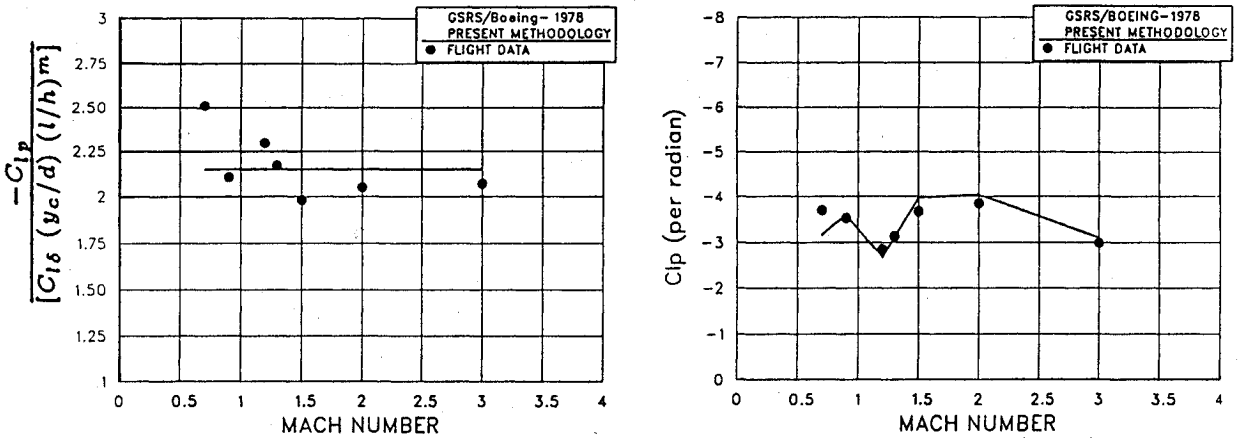

Fig. 8 Geometry, validation, and application to Boeing GSRS.

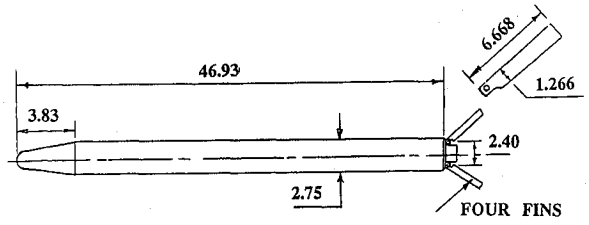

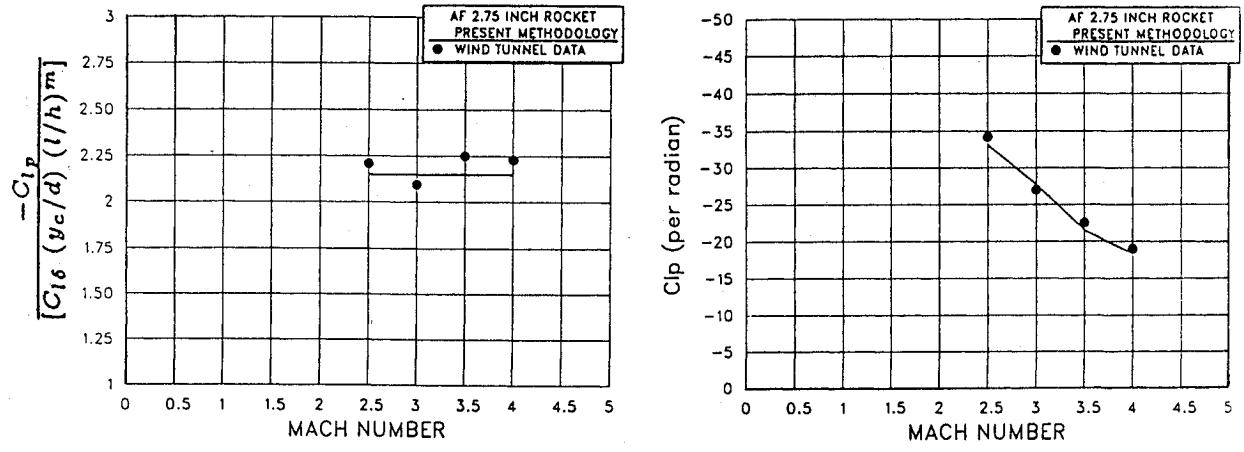

Fig. 9 Geometry, validation, and application to the Air Force 2.75-in. (70-mm) rocket.

version (not studied here) included a fin-tip bent of 20 deg to produce the same roll. Wind-tunnel data are given in Ref. 14. The numerical results of the tests are given in Table 6. The $C_{l\delta}$ values were adjusted to be per radian, rather per degree as given in Ref. 14. The correlation for the value 2.15 seems adequate, and the predicted C_{lp} values agree well with the data. The results are shown in Fig. 9.

G. Basic Finner Configuration

The early and familiar configuration of the 1950s was flight-tested in the range of the Ballistic Research Laboratory in about 1948–1949. It was a configuration approved by the U.S. Army, Navy, and Air Force at that time and is shown in Fig. 10. The range results are reported in Ref. 2. The configuration is a 10-caliber-long body with four flat simple fins. For this particular test the diameter was 0.785 in. (20 mm), with a sharp cone nose of 20 deg. Also for this particular test, only two of the four panels were canted. Seven models with different cant angles (2 and 4 deg) were tested and reported. The data given in Ref. 2 were per fin. Table 7 provides the data after adjusting the reference area and reference length to a standard body reference area and diameter, respectively, rather than the fin area and the fin span (including the body diameter), respectively, as is given in Ref. 2. Figure 10 shows the correlation constant, 2.15, to be very accurate. Also, the C_{lp} computed using Eq. (5) provides very good values in comparison with the data.

A comparison for the C_{lp} obtained by different methods was made for the Basic Finner case. First, C_{lp} was directly computed from the NSWC-AP code.[7] Second, it was computed using the correlation of Eq. (5) with $C_{l\delta}$ from the experimental range data. Third, C_{lp} was computed from Eq. (5) using $C_{l\delta}$ as computed from the fast approximate method presented in Sec. II.G. The comparison is made in Fig. 11, where the second method provided the best comparison with the experimental C_{lp} data. However, the first method using the NSWC-AP code proved less accurate than the method using the present simple evaluation scheme for $C_{l\delta}$. This result shows that the present method for calculation of $C_{l\delta}$ is quite adequate and reasonably accurate in comparison with the semiempirical methods or even the theoretical methods. This method is, however, limited to missiles with only one set of fins and to small angles of attack.

Finally, a compilation of all the cases considered, together with their experimental data, is given in Fig. 12 in comparison with the present extended correlation of Eq. (5). The compilation indicates excellent correlation.

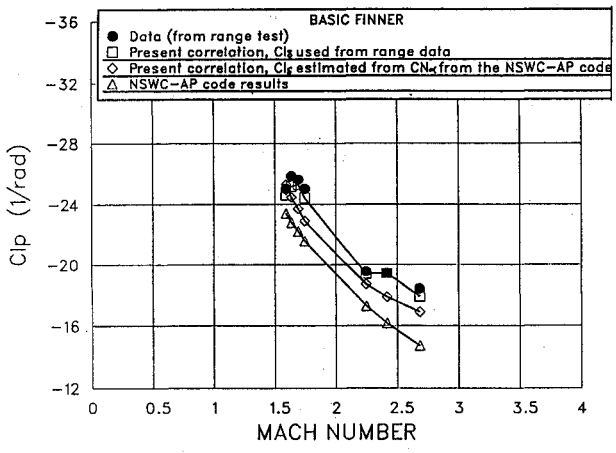

Fig. 11 Comparison for C_{lp} computed by different methods.

Table 6 Data and results for the AF 2.75-in. rocket

Mach number	$C_{l\delta}$ (data)	C_{lp} (data)	C_{lp} [Eq. (5)]
2.5	11.91	−34.2	−33.11
3.0	9.97	−27.0	−27.70
3.5	7.73	−22.5	−21.49
4.0	6.59	−19.0	−18.31

Table 7 Data and results for the Basic Finner projectile

Mach number	$C_{l\delta}$ (data)	C_{lp} (data)	C_{lp} [Eq. (5)]
1.59	11.98	−25.04	−24.60
1.64	12.26	−25.86	−25.17
1.69	12.32	−25.63	−25.29
1.75	11.89	−25.03	−24.41
2.25	9.44	−19.54	−19.38
2.42	9.46	−19.44	−19.42
2.68	8.71	−18.39	−17.88

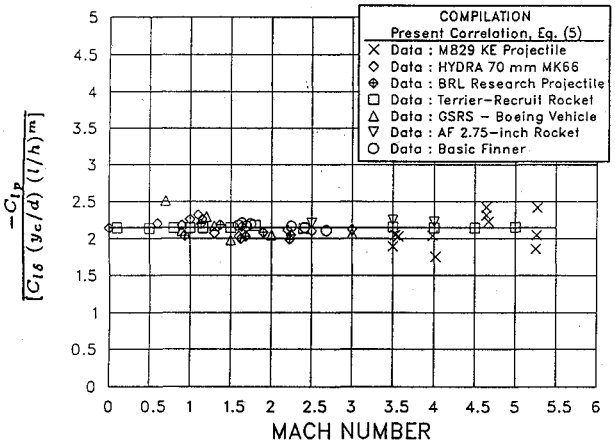

Fig. 12 Compilation of all data of all configurations.

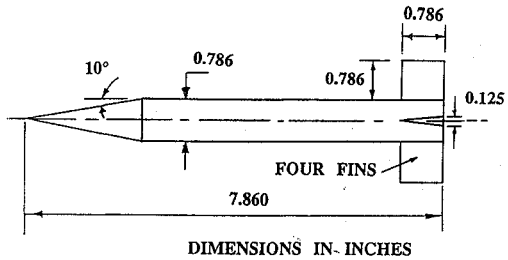

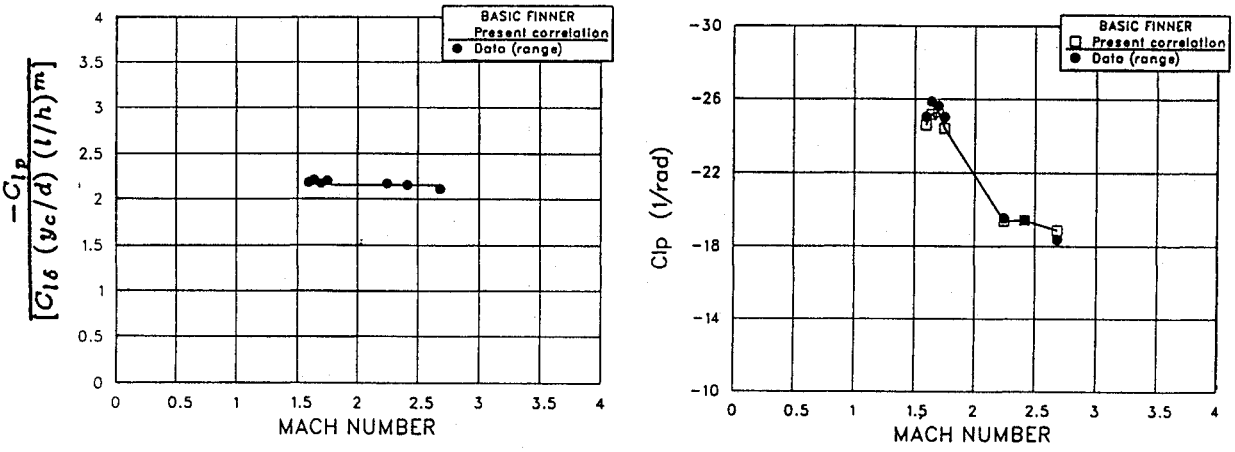

Fig. 10 Geometry, validation, and application to the Tri-Service Basic Finner projectile.

IV. Summary and Conclusions

The algebraic correlation of Eastman[1] has been extended to accept more finned missile/projectile configurations. The correlation relates the derivative of the roll-damping moment coefficient to that of the roll producing moment coefficient for the vehicle under study. The correlation was extended to accept arbitrary number of fins, curved wraparound canted fins, and configurations with offset fins. The correlation extension was based on and verified through experimental data on several different configurations. The correlation was found to be valid at subsonic, transonic, and supersonic speeds. The correlation is meant to be used to evaluate the more difficult coefficient C_{lp}, given $C_{l\delta}$. A simple method to evaluate $C_{l\delta}$ has been presented, using the more available coefficient C_N. This method proved to be even better than the lengthy semiempirical methods used in some fast aerodynamic prediction codes.

This surprisingly simple and apparently universal correlation reduces the number of costly full flowfield computations for such complex fin arrangements, if only C_{lp} is sought. It is suggested that new experimental data be applied further to the correlation to widen its application still further.

References

[1]Eastman, D. W., "Roll Damping of Cruciform-Tailed Missiles," *Journal of Spacecraft and Rockets*, Vol. 23, No. 1, 1986, pp. 119, 120.

[2]Bolz, R. E., and Nicolidas, J. D., "A Method of Determining Some Aerodynamic Coefficients from Supersonic Free-Flight Tests of a Rolling Missile," *Journal of the Aeronautical Sciences*, Vol. 17, Oct. 1950, pp. 609–621.

[3]Adams, G. J., and Dugan, D. W., "Theoretical Damping in Roll and Rolling Moment Due to Differential Wing Incidence for Slender Cruciform Wings and Wing–Body Combination," NACA Rept. 1088, 1958.

[4]Barrowman, J. S., Fan, D. N., Obosu, C. B., Vira, N. R., and Yang, R. J., "An Improved Theoretical Aerodynamic Derivatives Computer Program for Sounding Rockets," AIAA Paper 79-0504, 1979.

[5]Oberkampf, W. L., "Theoretical Prediction of Roll Moments on Finned Bodies in Supersonic Flow," AIAA Paper 77-111, Jan. 1974.

[6]Prakash, S., and Khurana, D. D., "A Simple Estimation Procedure of Roll Rate Derivatives for Finned Vehicle," *Journal of Spacecraft and Rockets*, Vol. 21, No. 3, 1984, pp. 318–320.

[7]Devan, L., and Mason, L. A., "Aerodynamics of Tactical Weapons to Mach Number 8 and Angle of Attack 180: Part II—Computer Program and User's Guide," NSWC-TR-81-358, Sept. 1981.

[8]Vukelich, S. R., Stoy, S. L., and Moore, M. E., "Missile DATCOM: Vol. II—User's Manual," Flight Dynamics Lab., AFWAL-TR-86-3091, Wright–Patterson AFB, OH, Dec. 1988.

[9]Weinacht, P., and Sturek, W. B., "Aerodynamics of the Roll Characteristics of the M829 Kinetic Energy Projectile and Comparison with Range Data," U.S. Army Ballistic Research Lab., BRL-TR-3172 (ADA233175), Aberdeen Proving Ground, MD, Nov. 1990.

[10]Dahlke, C. W., and Batiuk, G., "HYDRA 70 mm MK66 Aerodynamics and Roll Analysis," U.S. Army Missile Command, Rept. RD-SS-90-6, Redstone Arsenal, AL, July 1990.

[11]Kayser, L. D., "Aerodynamics of Fin-Stabilized Projectiles at Moderate Spin Rates," U.S. Army Ballistic Research Lab., BRL-MR-3965 (ADB163436), Aberdeen Proving Ground, MD, April 1992.

[12]Rollstin, L. R., "Aeroballistic Design and Development of the Terrier-Recruit Rocket System with Flight Test Results," Sandia Labs., Rept. SAND-74-0315, Albuquerque, NM, Jan. 1975.

[13]Monk, J. R., and Phelps, E. R., "GSRS Aerodynamic Analysis Report," Boeing Co., Document D328-10055-1, June 1978.

[14]Uselton, J. C., and Carman, J. B., "Wind Tunnel Investigation of the Roll Characteristics of the Improved 2.75-Inch-Diameter Folding Fin Aircraft Rocket at Mach Numbers From 2.5 to 4.5," Air Force Arnold Engineering Development Center, Rept. AEDC-TR-69-207, Arnold Air Force Station, TN, Nov. 1969.

Jerry Allen
Associate Editor